Int. J. Electrochem. Sci., 6 **(2011)** 1216 - 1229

International Journal of
ELECTROCHEMICAL
SCIENCE
www.electrochemsci.org

Study on the Cr^{3+}-Induced Ion Channel Based the Electron Transfer Rate Across Mimic Biomembrane Measured by Scanning Electrochemical Microscopy

Jianping Li[1,2*], *Xiaofei Jia*[1], *Yan Yan*[1], *Xuehong Zhang*[2]

1. College of Chemistry and Bioengineering, Guilin University of Technology, Guilin, 541004, China
2. The Guangxi Key Laboratory of Environmental Engineering, Protection and Assessment, Guilin, 541004, China
[*]E-mail: likianping@263.net

Received: 5 March 2011 / *Accepted:* 14 April 2011 / *Published:* 1 May 2011

To investigate the mechanism of Cr^{3+} ion translocation across the cell membranes, the interaction between the Cr^{3+} ion and the mimic biomembrane of solid supported lipid bilayer (s-BLM) has been investigated quantitatively. The mimic biomembrane was prepared according to the self-assemble of the phosphatidylcholiner(PC)/cholesterol(Ch) membrane on Pt electrode. Using ferricyanide anions species as a redox probe, cyclic voltammetric (CV), Alternating Current (A.C.) impedance spectroscopy (EIS), scanning electrochemical microscopy (SECM) and approach curves were measured. The apparent electron transfer rate constants between the surface of the electrode and redox species was independently calculated from the approach curve, which was measured by SECM, to prove quantitatively the model of the biomimic membrane interacted with Cr^{3+} in different concentration. The result showed that the apparent electron transfer rate constants increased as the concentration of Cr^{3+} attached to the surface of the s-BLM increased from 9.00×10^{-5} cm·s^{-1} to 1.02×10^{-2} cm·s^{-1} while the concentration of Cr^{3+} from 0 mg·L^{-1} to 780 mg·L^{-1} and two obvious platforms were observed at the constants of 9.3×10^{-4} cm·s^{-1} and 7.64×10^{-3} cm·s^{-1} respectively. The mechanism was suggested that Cr^{3+} ion interacted with the s-BLM and formed the ion-channels owing to the changes of the surface texture of the s-BLM, which resulted chromium ion translocation across mimic biomembrane by Cr^{3+} interaction with the Pt-BLM.

Keywords: Cr^{3+}, Ion channel, mimic biomembrane, SECM

1. INTRODUCTION

Owing to the trait of the strong remediation ability and the beneficial effect on the ecosystem, much attention has been paid to curb heavy metal pollution by using the technology of

phytoremediation since it had been proposed by Chaney firstly in 1977. The research on the accumulation mechanism of the hyper-accumulator has been receiving more and more attention. There are many researches about the accumulation mechanism of the heavy metal in the hyper-accumulator plants, which mainly focused on the changes in the content and the speciation of heavy metals in the inner and outer plant cell[1-3]. For example, the form and state of the heavy metal within the plant[4], as well as the absorption, transportation and stored procedures of the heavy metal had been analyzed by several approaches[5].

Because the cell membrane plays an important role in material exchange and information transmission, it is important to study the selective absorption process of metal ions in the hyper-accumulator plants to reveal the accumulation mechanism of heavy metal in the hyper-accumulator plants.

However, there were rare researches on the accumulation mechanism of the heavy metal in the hyper-accumulator plants about the metal ions transfer across the membrane[6-8]. *Leersia hexandra Sw.* is one of the hyper-accumulator plants which has the strong ability of chromium enrichment and has great artistic value in eliminating the chromium pollution[9]. We had already discussed the absorption characteristics of hexavalent chromium on the *Leersia hexandra Sw.* biomass[10,11]. The result showed that hexavalent chromium ion could be adsorbed on the *Leersia hexandra Sw*. biomass and reduced into trivalent chromium by the specific functional groups laid on the cell surface of the plants. To further investigate the absorption process of chromium ion by the hyper-accumulator plants, it is necessary to study the permeation processes of chromium ion into the plants cell and interaction between chromium ion and the cell membrane.

But the study on the ion permeation processes of the cell membrane in-situ was difficult because of the complexity of the component and the structure of the membrane of cell. In this paper, a biomimetic membrane system which has many similarities properties with cell membrane was used to investigate the interaction between the biomimetic membrane system and the trivalent chromium.

Many systems, including vesicles[12, 13], self-assembled monolayers[14], bilayer lipid membranes (BLM) and s-BLM[15-18] had been employed as the experimental platform of biomembrane in the interaction between ionic and membrane study. Among them, extensive studies were focused on the ion permeation processes facilitated by channel-forming peptides or ionophore[19-21], while relatively less qualitative research[22] has been carried out on the interaction between the ion and cell membrane.

The ion permeation processes facilitated by channel-forming peptides or ionophore usually involves two processes of electron transfer process of ion probe in BLM and the redox reactions between the BLM/electrolyte interface, which is benefit for electrochemical study. Due to the complicate process, not only the interfacial reactions involved, but also a problem about the matching of formal potentials of redox couples with that of probe, Tien[23] and his coworker reported the method of forming the s-BLM to act as mimic membrane and eliminated the redox reactions at BLM/electrolyte interface. Recently, by using this mimic membrane, Bard and his cooperators had presented a new theoretical methodology and discussed the electron transfer rate constants of redox probe through molecular monolayer and solid supported hybrid lipid bilayer membrane [16, 22, 24,

25]. However, to our knowledge, there were rare studies reported[26, 27] on which ions interacted with lipid membrane qualitatively, especially the utilization of SECM.

In the present study, the mimic biomembrane is prepared according to the self-assemble of the PC/Ch on Pt electrode, the SECM has been used to quantitatively investigate the apparent electron transfer rate constants of ferricyanide ions across the Pt-BLM under the interaction with Cr^{3+}, and a model was established to interpret the interaction between Cr^{3+} and the mimic membrane. The result is beneficial for the study the mechanism of Cr^{3+} across membrane.

2. EXPERIMENTAL

2.1. Chemical reagents

l-α-Phosphatidylcholine (PC) from fresh egg yolk and cholesterol (Ch) were purchased from Sigma (USA). $K_3Fe(CN)_6$, $K_4Fe(CN)_6$, $CrCl_3$, $CHCl_3$ and other chemicals were reagent grade and were used as received. All solutions were prepared with ultrapure water (18.2 MΩ·cm).

2.2. Formation of solid supported lipid bilayer membrane

The s-BLM was prepared according to the method described by Jiang[22]. A platinum disk electrode was firstly polished with 0.3 and 0.05 μm alumina, and sonicated in water for 10 min and then in acetone for 2 or 3 min. After cleaning the electrode with hot sulfuric acid and rinsing it with water, several scans were made over the range -0.3 ~ 1.5 V (*vs.* Ag/AgCl) in freshly prepared deoxygenated 1.0 mmol·L^{-1} H_2SO_4 on Pt electrode. The progress was repeated until the repetition CVs were got. The electrode was successively rinsed with water, then acetone, dried in pure nitrogen or argon. The s-BLM forming solution was prepared by taking 30 μL PC (2 mg·mL^{-1} in chloroform) and Ch (6 mg·mL^{-1} in chloroform) to form a uniformity admixture. Then, the mixture was dropped onto the Pt disk electrode surface and the electrode was immediately transferred to 0.1 mol·L^{-1} KCl bathing solution, in which the s-BLM formed spontaneously.

2.3. Scanning electrochemical microscopy measurements

All experiments included CV, SECM and Probe approach curve were carried out with the CHI 910B Scanning Electrochemical Microscopy (Chenhua Instrument Co., Shanghai, China), employing two three-electrode system with a tip ultramicroelectrode (UME, 10 μm diameter) and a Pt disk (2 mm diameter) working electrode, a platinum wire counter electrode and a Ag/AgCl reference electrode. The approach curves were obtained by setting the tip potential at 0.5V (*vs.* Ag/AgCl) and the substrate potential at -0.1V (*vs*. Ag/AgCl).

The approach speed of the tip to the substrate was 0.5 μm·s^{-1}. All experiments were carried out in a background solution containing 1.0 mmol·L^{-1} $K_3Fe(CN)_6$/$K_4Fe(CN)_6$ (molar ratio 1:1) and 0.1

mol·L^{-1} KCl at 25 $^{\circ}$C. The solutions were deaerated with purified nitrogen for at least 5 min to remove oxygen prior to the beginning of electrochemical measurements.

3. RESULTS AND DISCUSSION

3.1. The cyclic voltammetric study of the interaction between s-BLM and Cr^{3+} ions in different concentrations

The interaction between Cr^{3+} and the s-BLM modified Pt electrode was studied electrochemically with the aid of the hydrophilic species potassium ferrocyanide-potassium ferricyanide, because the mixture was usually used to probe an electrode modified by an thin layer and underwent a reversible, one-electron, outer-sphere redox reaction[28]. Fig. 1 shows the voltammograms of 1×10^{-3} mol·L^{-1} ferrocyanide/ferricyanide redox couple in 0.1 mol·L^{-1} KCl solution on Pt and BLM modified Pt-electrode.

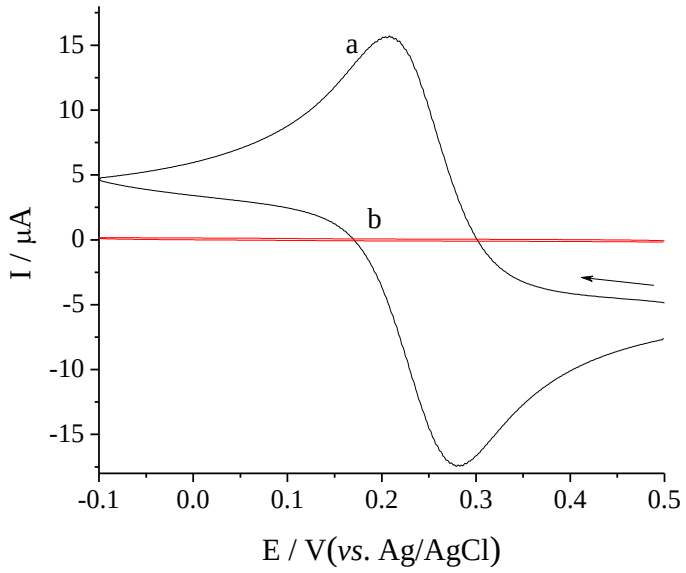

Figure 1. Cyclic voltammograms of 1×10^{-3} mol·L^{-1} ferrocyanide/ferricyanide anions in 0.1 mol·L^{-1} KCl solution on Pt electrode (a) and PC/Ch BLM modified Pt electrode (b); v=/0.05 V·s^{-1}

It can be seen from figure 1 that the currents decreased dramatically when the BLM was coated on the surface of Pt electrode. Curve (a) in Fig. 1 indicated that the probe of ferricyanide anions could freely reach to the surface of the Pt electrode and underwent redox reaction; The current of the curve (b), which was almost 1/10 of that in the curve (a), indicated that a well organized bilayer had formed and s-BLM had successfully been coated on the surface of the Pt electrode, then the densely packed bilayer acted as an effective barrier for potassium ferricyanide to approach the Pt electrode surface.

Fig. 2 shows the voltammograms of 1×10^{-3} mol·L^{-1} ferrocyanide/ferricyanide redox mediator on the s-BLM modified electrode in 0.1 mol·L^{-1} KCl after the s-BLM interacted with Cr^{3+} ions in different concentrations. The currents and potential difference between the anodic and the cathodic peaks increased with the increasing of Cr^{3+} concentrations which implied that the ion-channel formed due to the change of structure of the membrane and the ion probe could reach to the surface of the Pt electrode for the redox reaction.

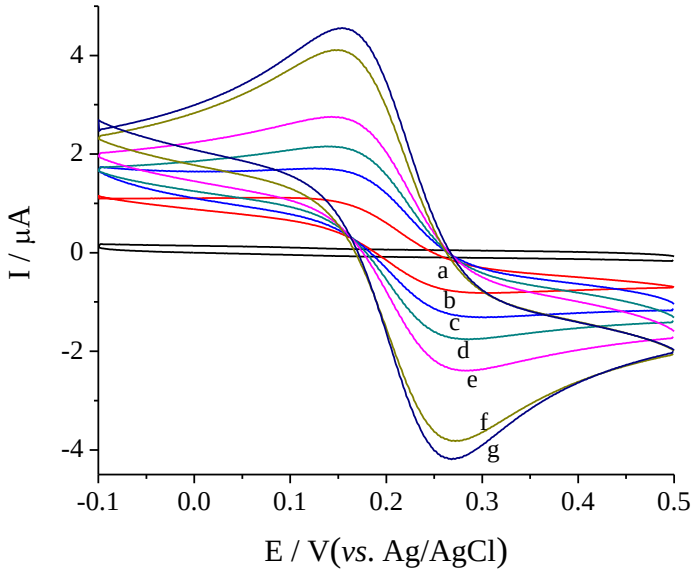

Figure 2. The cyclic voltammograms of 1×10^{-3} mol·L^{-1} ferrocyanide/ferricyanide anions on s-BLM modified electrode interacted with concentration of Cr^{3+} ion: 80 (a), 100 (b), 110 (c), 130 (d), 150 (e), 200 (f) and 400 (g) mg·L^{-1} in 0.1 mol·L^{-1} KCl; *v*=/0.05 V·s^{-1}

3.2. Characterization of BLM

The stability of the bilayer membrane on Pt electrode was assessed by recording the voltammograms of s-BLM modified electrode immersed in 1×10^{-3} mol·L^{-1} ferrocyanide/ferricyanide (in 0.1mol/L KCl) for different time.

Fig. 3 shows that the currents slightly increased during the 80 minutes, but the current changes were less than that in figure 2. It evidently proved that the s-BLM was relatively stable and suitable for the electrochemical measurement during the experiments. The insert in Fig. 2 demonstrated the voltammogrms of 1×10^{-3} mol·L^{-1} ferrocyanide/ferricyanide in 0.1 mol·L^{-1} KCl for repeat scans.

Cholesterol plays an important role in the formation of the lipid bilayer. It could increase the fatty acid chains to add the number of lecithin molecules per unit area of membrane and decreased amplitude of motion of the long axis which influences the osmotic permeability of phospholipid membranes. It also could improve the stability of BLM by change the solubility of short-chain hydrocarbons in the lipid bilayer. In addition, the interaction between BLM and Cr^{3+} should be altered by changing the binding sites. The effect of dosage of cholesterol in s-BLM forming solution was estimated and the results were shown in figure 4. It can be seen that when the ratio of cholesterol

versus PC was 1:3, the current reached a minimum value. It means a stable lipid bilayer with less amplitude of motion was formed and the redox mediator could be hindered to get the surface of the Pt electrode.

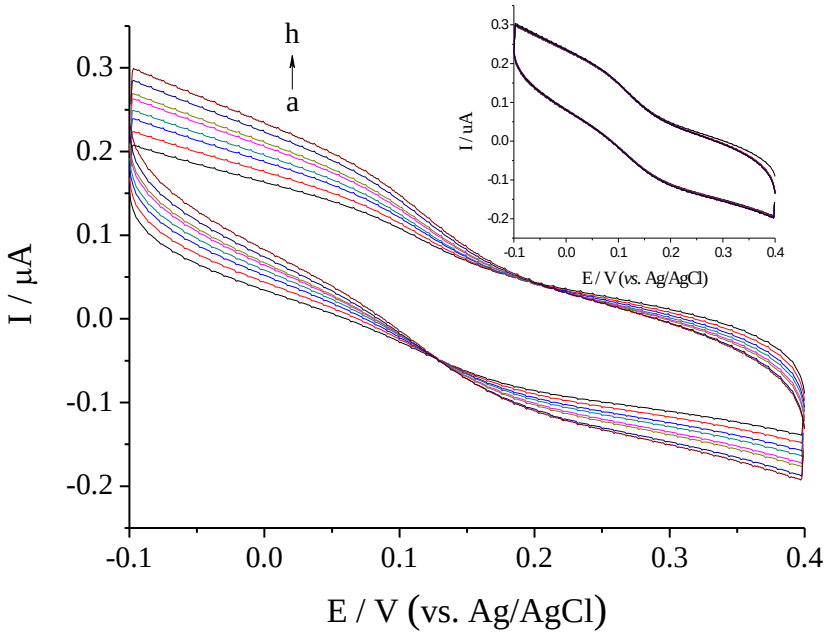

Figure 3. Cyclic voltammograms of BLM modified Pt electrode in 0.1 mol·L^{-1} KCl solution containing 1×10^{-3} mol·L^{-1} ferrocyanide/ferricyanide for 10 (a), 20 (b), 30 (c), 40 (d), 50 (e), 60 (f), 70 (g) and 80 (h) min; *v*=/0.05 V·s^{-1}, Cr^{3+}: 100 mg·L^{-1} The insert figure presents the curves of 15 scans after the BLM electrode immersed in solution for 30 min

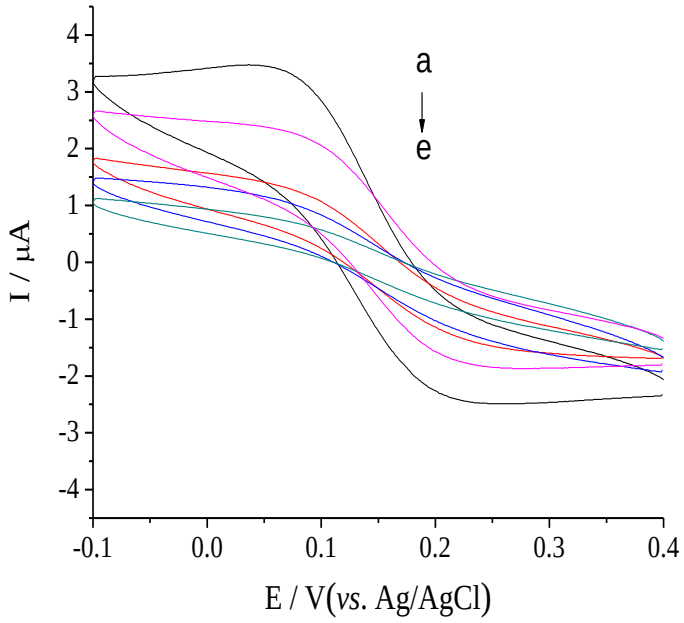

Figure 4. Cyclic voltammograms of 1×10^{-3} mol·L^{-1} ferrocyanide/ferricyanide anions in 0.1 mol·L^{-1} KCl solution on the Pt electrode modified with BLM fabricated in ratio of Ch and PC: 2:1(a), 1:2(b), 1:1(c), 1:4(d), and 1:3(e); *v*=/0.05 V·s^{-1}, Cr^{3+}: 100 mg·L^{-1}

3.3. A.C. impedance spectroscopy

A.C. impedance was used to monitor the interaction process between the modified electrode and Cr^{3+} ions. Fig. 5 shows that the Nyquist plots of the impedance spectra of the bare Pt electrode (a) and s-BLM modified electrode (b-e). When the s-BLM successfully assembled on the surface of Pt electrode, the diameter of the semicircle reached a maximum (e). After the modified electrode interacted with Cr^{3+} ions, the diameter of the semicircle gradually decreased with the increasing of Cr^{3+} concentration. The semicircle diameter in the impedance spectrum is approximately equal to the charge transfer resistance R_{CT}, which controls the electron transfer rate of the redox probe at the electrode interface. Therefore, curve (a) showed that ferricyanide anions could easily reach the electrode surface. When the s-BLM was coated on the surface of the Pt electrode, curve (e) indicated that densely packed bilayer acted as an effective barrier and the ion probe could not contact the electrode surface. When the concentration of Cr^{3+} ions gradually increased from 80 $mg \cdot L^{-1}$ (d) to 200 $mg \cdot L^{-1}$ (b), the interaction between Cr^{3+} and the acidic phosphate head group of the s-BLM increased, and the surface texture of the s-BLM changed. As a results, the electric conductivity of the s-BLM increased which led to the semicircle diameter in the impedance spectrum gradually decreased. The result is in agreement with previously measured by CV.

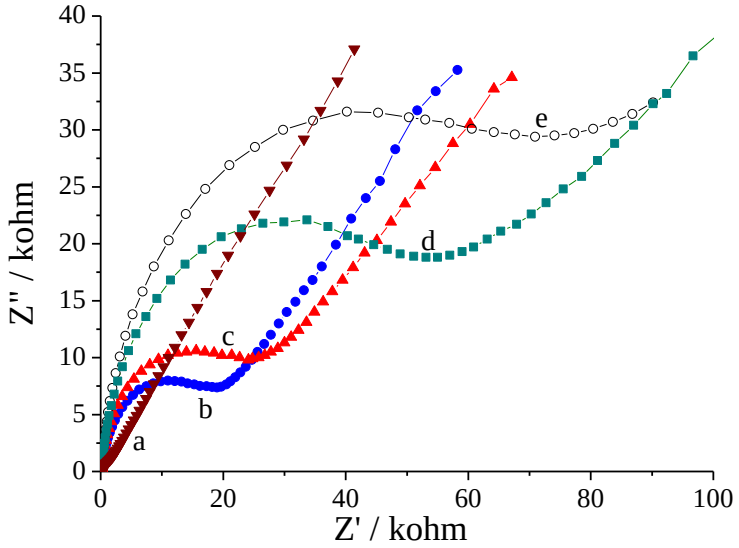

Figure 5. AC impedance spectra of Pt electrode (a) and BLM modified electrode interacted with Cr^{3+} ions in concentration of 0 (e), 80 (d), 130 (c) and 200 (b) $mg \cdot L^{-1}$ in 1×10^{-3} $mol \cdot L^{-1}$ ferrocyanide/ferricyanide anions and 0.1 $mol \cdot L^{-1}$ KCl; frequency range: 0.1-10^5 Hz

3.4. SECM images of s-BLM on Pt electrode

SECM is a powerful method for imagine the electrode surface and has been extensively used to characterize self-assembled layers, acquire topographics of the substrates and distinguish the differences of the electrode surface. Figure 6a and b display the 3D contour plots for surface of the Pt electrode and the s-BLM modified Pt electrode. Figure 6c and d are the plots for surface of Pt-BLM after interaction with Cr^{3+} (100 $mg \cdot L^{-1}$) for 30 and 60 min, respectively. It could find that the surface

of Pt-BLM electrode is uniform and dense, showing lower current. An undulant and irregular currents surface was shown in figure 6c due to the changes of BLM structure when exposed to Cr^{3+} solutions. The observed results were also time-dependent which was shown in figure 6d. Considering to the stability of the BLM, we take the 30 min as the further analyses.

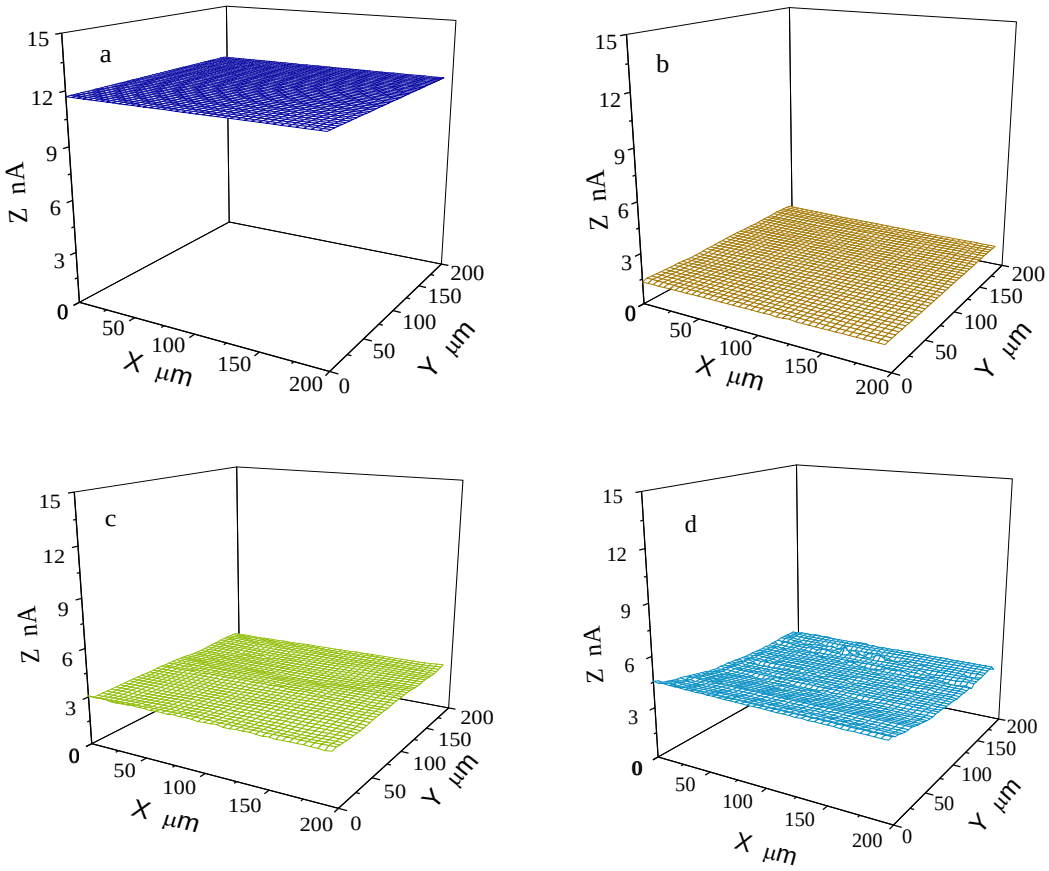

Figure 6. SECM images of Pt electrode and Pt-BLM electrode in 1.0 mmol·L^{-1} ferrocyanide/ ferricyanide anions containing 0.1 mol·L^{-1} KCl; a) Pt electrode; b) Pt-BLM electrode; c) Pt-BLM electrode interaction with Cr^{3+} (100 mg·L^{-1}) for 30 min; d) Pt-BLM electrode interaction with Cr^{3+} (100 mg·L^{-1}) for 60 min

3.5. The model of s-BLM interacted with the Cr^{3+} ion

The infrared spectroscopy was used to monitor the interconversion of structural information of the BLM reacted with Cr^{3+}. The Fig. 7 shows the infrared spectrum of the BLM in the absence (a) and presence (b) of Cr^{3+}. In the presence of Cr^{3+}, the obvious changes occurred in the position of P=O and P-O-C bending vibration, 1240cm^{-1} and 1060cm^{-1}, respectively. The intensity at 1240cm^{-1} obviously decreased. The reason is that the acidic phosphate head group with the negatively charged had an interaction with the Cr^{3+} and reduced the dipole moment. The red-shift has taken place on the band 1060cm^{-1}. The changes in peak positions of P=O and P-O-C bending vibration indicate that there are electrostatic interactions between the BLM and the Cr^{3+}.

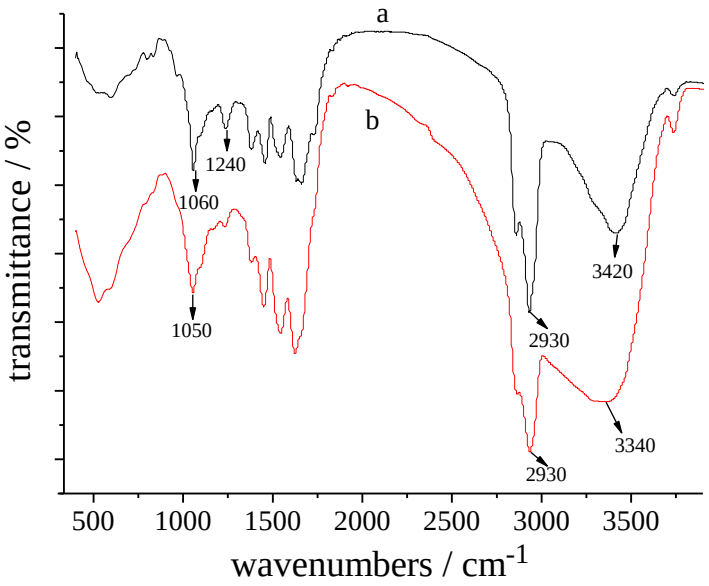

Figure 7. Infrared spectra of the BLM before (a) and after (b) reaction with Cr^{3+} ion

Based on the mechanism of ion channel proposed by Sugawara[29], the explanations of the current changes could be suggested that there were acidic phosphate head groups on the s-BLM and the surface texture of s-BLM would be changed when its' negatively charged acidic phosphate head groups were interacted with the Cr^{3+}. A drastic change in the alignment of molecular assembly of PC on Pt surface was expected by the interaction with the Cr^{3+}. There are three possible paths formed during the ferricyanide anions crossing s-BLM when Cr^{3+} interacted with the s-BLM, and the formation of ions channel was shown in Fig. 8. The three paths were presented as (1) The electron tunneling across bilayer of s-BLM; (2) Electron tunneling across monolayer; (3) Electron transfer between ferricyanide anions and the surface of Pt substrate electrode through Cr^{3+}-induced ion channels.

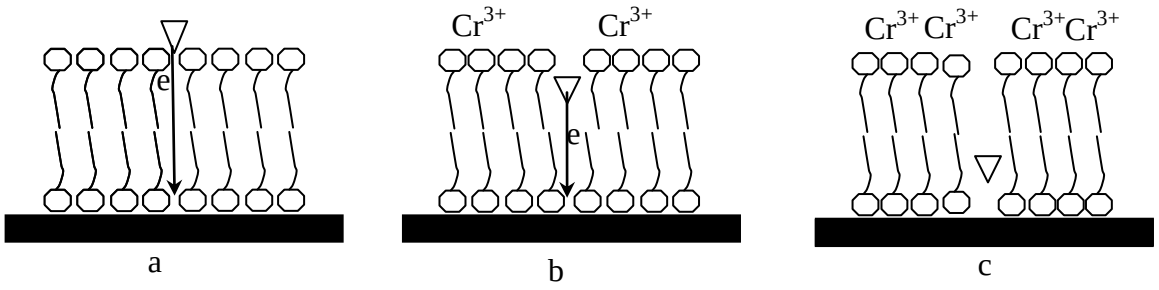

Figure 8. Schematic representation for three possible paths during ferricyanide anions crossing s-BLM when Cr^{3+} interacted with s-BLM in 1×10^{-3} mol·L^{-1} ferrocyanide/ferricyanide anions and 0.1 mol·L^{-1} KCl solution containing Cr^{3+} ions; a) electronic tunneling across bilayer; b) electronic tunneling across monolayer; c) electron transfer between ferricyanide anions and the surface of Pt substrate electrode through Cr^{3+}-induced ion channels. "▽" Represents ferricyanide anions

According to the model, it can be interrupted about the current altering in the presence of Cr^{3+} in different concentrations. In the absence of Cr^{3+}, the path of the ferricyanide ions transfer on the s-BLM was dominated chiefly in form of the electronic tunneling across bilayer (Fig. 8a). Due to the barrier of the modified membrane, there are only few ferricyanide ions transfer across bilayer of s-BLM and the current of modified electrode was relative less, only 6.1×10^{-7} A. In the contrary, with the increasing of Cr^{3+} concentration, the current gradually increased because Cr^{3+} interacted with the acidic phosphate head group of s-BLM and the surface texture of s-BLM get changed. When the concentration of Cr^{3+} was at a low concentration (39 $mg\cdot L^{-1}$), the tensile force on the acidic phosphate head group of s-BLM was relatively less and the interaction could be ignored. Therefore, the monolayer membrane ion channel (Fig. 8b) only formed, instead of the Cr^{3+}-induced ion channels (Fig. 8c) and the electron tunneling across monolayer (Fig. 8b) became the main path of ferricyanide ions transfer in this moment. Finally, when the concentration of Cr^{3+} ions was gradually increased from 52 $mg\cdot L^{-1}$ to 780 $mg\cdot L^{-1}$, more Cr^{3+} interacted with the acidic phosphate head group of the s-BLM, the tensile force on s-BLM was so large that the ion channels induced by Cr^{3+} (Fig. 8c) formed. The electron transfer between ferricyanide anions and the Pt substrate electrode through Cr^{3+}-induced ion channels (Fig. 8c) became the main path. Therefore, the ferricyanide ions crossed the s-BLM for redox reaction and the current gradually increased with the increasing of Cr^{3+} concentration.

3.6. The apparent rate of heterogeneous electron transfer consent between the surface of the electrode and redox probe

Aiming to prove the interaction process between the Cr^{3+} and the s-BLM modified electrode, the apparent electron transfer rate constants of ferricyanide ions in the model shown in Fig. 8 were measured by the SECM.

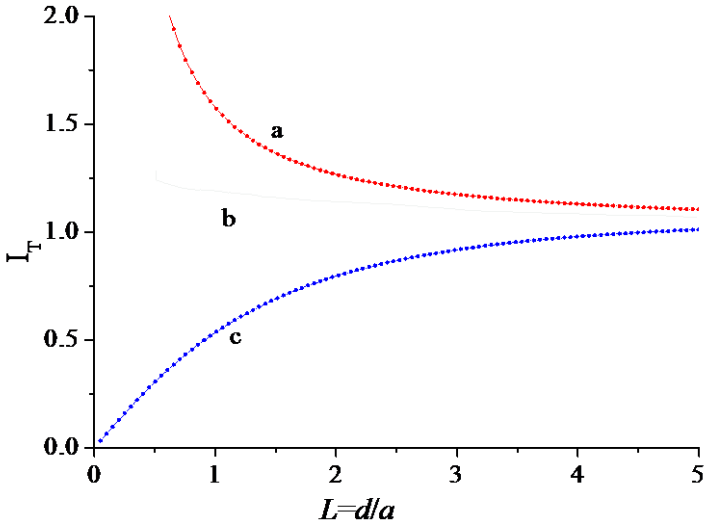

Figure 9. Current-distance curves for a 5 μm-radius Pt tip UME approaching; (a) the Pt electrode; (b) Pt-BLM electrode; (c) the insulating substrate. The tip was biased at 0.5 V (*vs*. Ag/AgCl) and the substrate at -0.1V (*vs*. Ag/AgCl) in 1×10^{-3} $mol\cdot L^{-1}$ ferrocyanide/ferricyanide solution containing 0.1 $mol\cdot L^{-1}$ KCl. The tip scan rate was 0.5 $\mu m\cdot s^{-1}$.

It gave a vigorous proof on the quantitative side about the interaction between the s-BLM modified electrode and the Cr^{3+}. The apparent rates can be determined with high lateral resolution while scanning a tip parallel to the surface. In this paper, SECM was used as an approach measure to characterize the electron transfer processes occurring at the surface of s-BLM modified electrode interacted with Cr^{3+} in different concentrations. The tip potential was 0.5 V to generate the $[Fe(CN)_6]^{3-}$ and the substrate potential was held at -0.1 V to reduce $[Fe(CN)_6]^{3-}$ back to be $[Fe(CN)_6]^{4-}$.

Fig. 9 shows the approve curves obtained with the substrate electrode of Pt electrode(a), s-BLM modified Pt electrode (b) and the insulating substrate (c). In the figure, *d* is the distance between the substance to the tip electrode and *a* is the radius of the tip electrode. When the Pt UME tip approached to the bare Pt electrode (the conductive substrate), the redox species could freely reach to the surface of the tip UME to generate $[Fe(CN)_6]^{3-}$ and then reach to the surface of the conductive substrate and reduce back to be $[Fe(CN)_6]^{4-}$ to form a positive-feedback curve. However, when the Pt substrate covered by the BLM, only few $[Fe(CN)_6]^{3-}$ could reached to the surface of the substrate electrode to be reduced back to $[Fe(CN)_6]^{4-}$, the current would be gradually decreased. So the current-distance curves would become the negative-feedback curve when the insulating substrate was used.

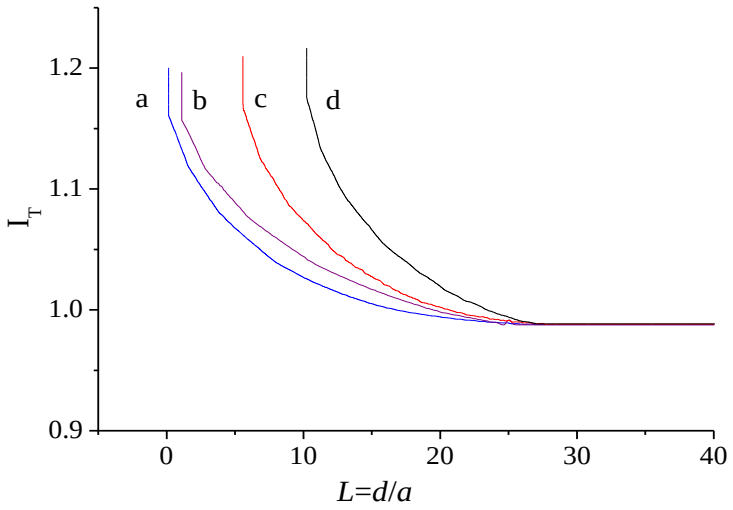

Figure 10. Current-distance curves for the BLM modified electrode interacted with different concentration of Cr^{3+} ions: 110 (a), 130 (b), 150 (c) and 780 (d) $mg \cdot L^{-1}$. The tip was biased at 0.5 V (*vs.* Ag/AgCl) and the substrate at -0.1V (*vs.* Ag/AgCl) in 1×10^{-3} $mol \cdot L^{-1}$ ferrocyanide/ferricyanide anions solution containing 0.1 $mol \cdot L^{-1}$ KCl. The tip scan rate was 0.5 $\mu m\ s^{-1}$

Fig. 10 shows that the approve curves obtained with the s-BLM modified electrode interacted with Cr^{3+} in different concentration. When Cr^{3+} concentration changed from 110 $mg \cdot L^{-1}$ to 780 $mg \cdot L^{-1}$, the surface texture of the lipid bilayer membrane would be changed and ferricyanide anions could finally and freely reach to the surface of the substrate to be reduced back as ferrocyanide anions. The normalized current was clearly increasing at the same normalized distance, such as curve (a) to curve (d). In other words, the apparent electron transfer rate of ferricyanide ions increased as the

concentration of Cr^{3+} ion attached solid supported lipid bilayers increasing. This is also in agreement with that measured by CV and EIS.

In order to obtain the apparent electron transfer rate constants of the ferricyanide ions under different concentration of Cr^{3+} ions, the expression of the tip current was given as a function of the normalized tip-substrate separation ($L=d/a$)[15, 24] as：

$$I_{\mathrm{T}}^{\mathrm{k}} = [\frac{0.78377}{L(1+1/\Lambda)} + \frac{0.68+0.3315\exp(-1.0672/L)}{1+F(L,\Lambda)}] \times (1 - I_T^{ins}/I_T^c) + I_T^{ins} \quad (1)$$

$$\mathrm{I}_{\mathrm{T}}^{\mathrm{c}} = 0.78377/L + 0.3315\exp(-1.0672/L) + 0.68 \quad (2)$$

$$I_T^{ins} = 1/(0.15 + 1.5358/L + 0.58\exp(-1.14/L) + 0.0908\exp[(L-6.3)/(1.017\mathrm{L})]) \quad (3)$$

$$\Lambda = \mathrm{kd/D} \quad (4)$$

$$F(L,\Lambda) = (11+7.3\Lambda)/\Lambda/(110-40L) \quad (5)$$

Where I_T^c and I_T^{ins} represent the tip currents of conductive and insulating substrates, respectively; k is the apparent limiting heterogeneous rate constant and D the diffusion coefficient (D = 7.6×10^{-6} cm^2 s^{-1}).

Figure 11 gives the dependence of Cr^{3+}concentration on the apparent electron transfer rate constants of the ferricyanide ions.

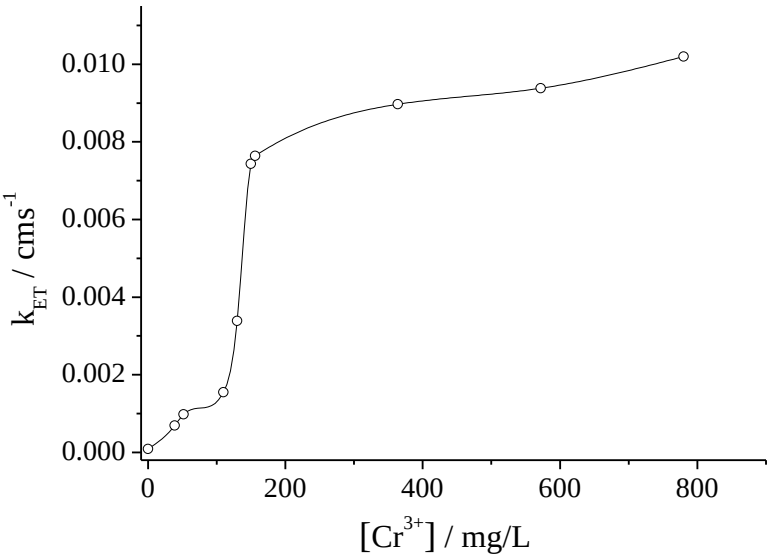

Figure 11. Dependence of Cr^{3+}concentration (0, 39, 52, 110, 130, 150, 156, and 780 $mg\cdot L^{-1}$) on the apparent electron transfer rate constants of the ferrocyanide/ferricyanide anions

There were two obvious platforms observed at the apparent electron transfer rate constants, 9.3×10^{-4} cm·s^{-1} and 7.64×10^{-3} cm·s^{-1} respectively. When the Cr^{3+} concentration was lower and no interaction with the surface of the mimic biomembrane occurred, the rate of the electron transfer was only 9.00×10^{-5} cm·s^{-1} because of the barrier of the modified membrane. From the platforms it can be demonstrated that the paths of electron transfer on s-BLM is dominated chiefly in form of the electronic tunneling across the bilayer (Fig. 8a). After the mimic biomembrane interacted with the Cr^{3+} ions in relatively lower concentration (39 mg·L^{-1}), the tensile force on the surface of the modified membrane was smaller and the Cr^{3+} induced ion channel was hardly formed and the apparent electron transfer rate constants increased slightly to be 4.93×10^{-4} cm·s^{-1}, which was in agreement with 4.1×10^{-4} cm·s^{-1} measured by Bard[15]. In this case, the path of ferricyanide ions transfer on s-BLM was dominated chiefly in form of the electronic tunneling across monolayer (Fig. 8b). When the Cr^{3+} concentration was high than 110 mg·L^{-1}, the apparent rate would increase markedly, and the second platform was obtained with the apparent rate increasing from 1.55×10^{-3} cm·s^{-1} to 1.02×10^{-2} cm·s^{-1}. The Cr^{3+}-induced ion channels on the surface of Pt electrode (Fig. 8c) had became the main path of ferricyanide ions transfer on the s-BLM, and ferricyanide anions would cross the s-BLM to complete the redox reaction.

4. CONCLUSIONS

The results showed that there were interaction between Cr^{3+} and the s-BLM self-assembled on Pt electrode by the tensile force on the acidic phosphate head group of s-BLM to form the Cr^{3+}-induced ion channels. When the concentration of Cr^{3+} ions was increased to 780 mg·L^{-1}, the Cr^{3+} ions induced ion channels could be formed. It might give the proof for the absorption of chromium ions by the cell of hyper-accumulator plants. The further studies on the selective trans-membrane of s-BLM in the presence of Cr^{3+} ions to identify the selective absorption of chromium ions is in studying and the results will be reported soon.

ACKNOWLEDGEMENTS
This work is supported by the Nature Science Foundation of China (20665003).

References

1. Z.G. Wei, J.W.C. Wong, H.Y. Zhao, H.J. Zhang, H.X. Li and F. Hu, *Bio. Trace Elem. Res.*, 118 (2007) 146
2. R.S. Boyd and E.M. Jhee, *Chemoecology.*, 15 (2005) 179
3. M.A. Klein, H. Sekimoto, M.J. Milner and L.V. Kochian, *Plant Physiol*., 147 (2008) 2006
4. H.L. Xie, R.F. Jiang, F.S. Zhang, S.P. McGrath and F.J. Zhao, *Plant Soil*., 318 (2009) 205
5. D.E. Salt, R.C. Prince, A.J.M. Baker, I. Raskin and I.J. Pickering, *Environ. Sci. Technol*., 33 **(**1999) 713
6. Y. Kobae, T. Uemura, M.H. Sato, M. Ohnishi, T. Mimura, T. Nakagawa and M. Maeshima, *Plant Cell Physiol*., 45 (2004) 1749

7. S. Puig, N. Andres-Colas, A. Garcia-Molina and L. Penarrubia, *Plant Cell Environ*., 30 (2007) 271
8. U. Krämer, I.N. Talke and M. Hanikenne, *FEBS Lett*., 581(2007) 2263
9. X.H. Zhang, J. Liu, H.T. Huang, J. Chen, Y.N. Zhu and D.Q. Wang, *Chemosphere*., 67 (2007) 1138
10. J.P. Li, Q.Y. Lin, X.H. Zhang and Y. Yan, *J. Colloid Interf. Sci*., 333 (2009) 71
11. J.P. Li, Q.Y. Lin and X.H. Zhang, *J. Hazard. Mater*., 182 (2010) 598
12. T. Heimburg, A. Blicher, K. Wodzinska, M. Fidorra and M. Winterhalter, *Biophys. J.* 96(2009) 4581
13. H. Patel, C. Tscheka and H. Heerklotz, *Soft Matter*, 5(2009) 2849
14. Z. Q. Feng, S. Imabayashi, T. Kakiuchi and K. Niki, J. Chem. Soc., Faraday Trans., 93 (1997) 1367
15. B. Liu, A.J. Bard, M.V. Mirkin and S.E. Creager, *J. Am. Chem. Soc*., 126 (2004) 1485
16. E.T. Castellana and P.S. Cremer, *J. Surf. Sci. Rep.*, 61 (2006) 429
17. H. Zhang, Z. Zhang, J. Li, and S. Cai, *Int. J. Electrochem. Sci*., 2 (2007) 788
18. X. Lu, T. Liao, L. Ding, X. Liu, Y. Zhang, Y. Cheng and J. Du, *Int. J. Electrochem. Sci*., 3 (2008) 797
19. X. Han, Y. Tong, W. Huang and E. Wang, *J. Electroanal. Chem*., 523(2002) 136
20. T. Heimburg, *Biophys. Chem.*, 150 (2010) 2
21. T. Janas, H. Krajiński and T. Janas, *Biophys. Chem.*, 7 (2000) 167
22. D.L. Jiang, P. Diao, R.T. Tong, D.P. Gu and B. Zhong, *Bioelectrochem. Bioenerg.*, 44 (1998) 285
23. H.T. Tien and A.L. Ottova, *Electrochim. Acta.*, 43 (1998) 3587
24. C. Cannes, F. Kanoufi and A.J. Bard, *J. Electroanal. Chem*., 547 (2003) 83
25. M.P. Jensen, J.A. Dzielawa, P Rickert and M.L. Dietz, *J. Am. Chem. Soc*., 124 (2002) 10664
26. A.A. Gurtovenko and I. Vattulainen, *Biophys. J*., 92 (2007) 1878
27. M. Przybyło, A. Olżyńska, S. Han, A. Ożyhar and M. Langner, *Biophys. Chem*., 129 (2007) 120
28. J. Weber, Z. Samec and V. Marecek, *J. Electroanal. Chem*., 94 (1978) 169
29. M. Sugawara, K. Kojima, H. Sazawa and Y. Umezawa, *Anal. Chem*., 59 (1987) 2842